Title

NFM Cross-Reactivity to MOG Does Not Expand a Critical Threshold Level of High-Affinity T Cells Necessary for Onset of Demyelinating Disease

Journal

The Journal of Immunology, 199(8)

ISSN

0022-1767

Authors

Blanchfield, Lori
Sabatino, Joseph J
Lawrence, Laurel
et al.

Publication Date

2017-10-15

DOI

10.4049/jimmunol.1700792

Peer reviewed

HHS Public Access

Author manuscript

J Immunol. Author manuscript; available in PMC 2018 October 15.

Published in final edited form as:

J Immunol. 2017 October 15; 199(8): 2680–2691. doi:10.4049/jimmunol.1700792.

NFM cross-reactivity to MOG does not expand a critical threshold level of high affinity T cells necessary for onset of demyelinating disease

Lori Blanchfield[1], **Joseph J. Sabatino Jr.**[2], **Laurel Lawrence**[1], and **Brian D. Evavold**[3]

[1]Department of Microbiology and Immunology, Emory University, Atlanta, GA 30322

[2]Department of Neurology, University of California, San Francisco, CA 94158

[3]Division of Microbiology and Immunology, Department of Pathology, University of Utah, Salt Lake City, UT 84112

Abstract

Of interest to the etiology of demyelinating autoimmune disease is the potential to aberrantly activate $CD4^+$ T cells due to cross-recognition of multiple self-epitopes such as has been suggested for MOG_{35-55} and NFM_{15-35}. $NFM_{15-35}$is immunogenic in C57BL/6 mice but fails to induce demyelinating disease by polyclonal T cells despite having the same TCR contact residues as MOG_{35-55}, a known encephalitogenic antigen. Despite reported cross-reactivity with MOG specific T cells, the polyclonal response to NFM_{15-35} did not expand threshold numbers of MOG_{38-49} tetramer positive T cells. Furthermore, NFM lacked functional synergy with MOG to promote EAE because $NFM^{-/-}$ mice developed an identical disease course to wild type mice after challenge with MOG_{35-55}. Single cells analysis of encephalitogenic T cells using the pMHC monomer based 2D micropipette adhesion frequency assay confirmed that NFM was not a critical antigen driving demyelinating disease because NFM_{18-30} specific T cells in the CNS were predominantly reactive to MOG_{38-49}. The absence of NFM contribution to disease allowed mapping of the amino acids required for encephalitogenicity and expansion of high affinity, MOG specific T cells that defined the polyclonal response. Alterations of N-terminal residues outside of the NFM_{15-35} core nonamer promoted expansion of high affinity, MOG_{38-49} tetramer positive T cells and promoted consistent EAE induction, unlike mice challenged with NFM_{15-35}. While NFM_{15-35} is immunogenic and cross-reactive with MOG at the polyclonal level, it fails to expand a threshold level of encephalitogenic, high affinity MOG specific T cells.

Introduction

Myelin specific T cells exist in all individuals, but it is not clear how these cells initially become triggered to attack self and promote autoimmune disease (1). Multiple factors influence the autoimmune T cell response which can be shaped by positive and negative

Address correspondences to Dr. Brian D. Evavold, University of Utah, Department of Pathology, 15 North Medical Dr. East, Rm 5200, Salt Lake City, UT 84112. brian.evavold@path.utah.edu.

This article was conceptually designed and interpreted in collaboration between LB, JS and BE. The paper was written by LB and critically reviewed and edited by JS and BE. Data was generated by LB, JS and LL.

selection pressures in the thymus and periphery (2, 3), genetic predispositions (4), environmental exposures (5), ability to migrate to the CNS and differentiation into effector and memory subsets (6). Central to these factors is how the TCR sees self-peptides presented on MHC, with MHC being the strongest genetic susceptibility factor currently identified for multiple sclerosis (7-9). One hypothesis for activation of autoreactive T cells is that exposure to structurally related / cross reactive peptides derived from self or foreign origins can break tolerance (10-13). $CD4^+$ T cell cross-recognition between MOG_{35-55} (myelin oligodendrocyte glycoprotein epitope 35-55) and NFM_{15-35} (epitope 15-35 of neurofilament medium protein) in demyelinating autoimmunity is of interest for disease etiology because these two self-epitopes have synergist potential as targets of autoimmune T cell attack due to identical amino acids at proposed TCR contacts (14). Conceptually, T cell recognition and responsiveness to multiple peptides is a critical feature of protective immune surveillance where a limited TCR repertoire is presented with a myriad of peptides displayed on MHC (15-17). In one example, a single T cell clone specific for myelin basic protein (Ac1-11) has the potential to recognize 10^6 peptides generated from a combinatorial library (18).

Physical interactions between TCR and peptide:MHC (pMHC) provide another level of input for understanding the initiation of TCR signaling. T cell cross-reactivity is unique to the amino acid structure of an individual TCR dictating how it physically recognizes peptides oriented within MHC (19). Alterations in peptides at amino acid residues interfacing with the TCR, known as altered peptide ligands (APL), can change the functional outcome of T cell responses (12, 18, 20-22) by changing affinity of the TCR:pMHC interaction as well as binding kinetics, including on / off rates and bond lifetime (23, 24). Associations between affinity and function of T cells contributing to polyclonal, demyelinating autoimmune disease have identified a breadth of high and low affinity interactions between TCR and pMHC in C57BL/6 and NOD models (25-27). Our goal is to understand how cross-recognition, cross-reactivity and biophysical interactions, such as 2D affinity, define onset of demyelinating autoimmunity in polyclonal models.

The study of polyclonal T cell cross-reactivity to MOG_{35-55} and NFM_{15-35} is a novel platform to study the etiology of demyelinating autoimmune disease. Currently, polyclonal studies examining T cell specificity to MOG and NFM do not paint a clear model for cross-reactivity and disease because NFM involvement is based on functional responses after MOG_{35-55} and not NFM_{15-35} priming (28). While this experimental approach stems from earlier reports stating NFM_{15-35} does not induce EAE (14), we questioned why this would be the case and chose to comparatively track antigen specific T cells after a MOG_{35-55} or NFM_{15-35} challenge.

We demonstrate that lack of EAE onset after NFM_{15-35} challenge correlated with insufficient expansion of high affinity, MOG_{38-49} tetramer positive T cells in spleen and peripheral lymph nodes along with their absence in the CNS. 2D micropipette adhesion frequency assay was used as a more sensitive, monomer based tool to enhance detection of TCR affinity and antigen specificity above tetramer staining in order to tease apart the bispecific $CD4^+$ T cell infiltrates in the CNS that are predominantly low affinity and fail to stain with tetramer (25). After MOG_{35-55} challenge we found that the CNS T cell infiltrates

recognizing NFM_{18-30} largely cross-recognized MOG_{38-49} and generally lacked the higher affinity cells typically seen with MOG_{38-49} specific infiltrates. The functional requirement of MOG and NFM bispecific T cells to EAE onset and severity was tested with MOG_{35-55} challenge of $NFM^{-/-}$ mice. This design revealed MOG and not NFM to be the critical autoantigen for EAE because $NFM^{-/-}$ mice developed a similar disease course to wild type, NFM sufficient mice. Furthermore, we mapped N-terminal residues of NFM_{15-35} that dictated poor encephalitogenicity such that when modified allowed EAE induction as well as detection of MOG_{38-49} tetramer positive T cells. The presented data concomitant with the fact that $MOG^{-/-}$ mice do not develop EAE after MOG_{35-55} or NFM_{15-35} challenge (29) supported the conclusion that NFM has a minimal role in the onset of EAE and the expansion of encephalitogenic T cells from the polyclonal repertoire where pathogenicity is dictated by expansion of a critical threshold level of higher affinity tetramer positive MOG specific T cells.

Materials and methods

Mice

Female C57BL/6 mice were purchased from Charles River Frederick Facility, formerly National Cancer Institute (NCI). With permission from Dr. Hugh Reid at Monash University, $MOG^{-/-}$ mice (29) were obtained from Dr. Xue-Feng Bai at The Ohio State University. $NFM^{-/-}$ mice were obtained from Dr. Julien (30) and backcrossed to NCI C57BL/6N mice due to visual dominance of the 129 background coat color and the presence of an additional *nefh* knockout. Completion of the backcross was confirmed by DartMouse (Lebanon, NH) and NFM protein deficiency was determined by histology performed at Emory NINDS Neuropathology / Histochemistry Core Facility (Atlanta, GA). $IFN\gamma R^{-/-}$ (B6.129S7-*Ifngr1*^{tm1Agt}/J) mice, Thy1.1 mice (B6.PL-*Thy1*^{a}/CyJ), and 2D2 transgenic mice (C57BL/6-Tg(Tcra2D2,Tcrb2D2)1Kuch/J) were initially purchased from Jackson Laboratories. These mice along with SMARTA (Tg(TcrLCMV)Aox) mice (31) were all housed in the Division of Animal Resources at Emory University and handled in accordance with protocols approved by the Institutional Animal Care and Use Committee. Experimental mice were between 6-11 weeks of age.

Peptides and reagents

Peptides used for T cell priming and EAE induction were generated in our laboratory with the Prelude peptide synthesizer (Protein Technologies, Inc) with the following sequences; MOG_{35-55} (MEVGWYRSPFSRVVHLYRNGK), NFM_{15-35} (RRVTETRSSFSRVSGSPSSGF), NFM_{15-35} T20Y (RRVTE**Y**RSSFSRVSGSPSSGF), NFM_{15-35} E19W, T20Y (RRVT**WY**RSSFSRVSGSPSSGF), NFM_{15-35} S23P (RRVTETRS**P**FSRVSGSPSSGF), NFM_{15-35} S28V (RRVTETRSSFSRV**V**GSPSSGF).

Lymph node priming and T cell proliferation assays

Polyclonal T cell lines were generated by footpad priming mice with emulsions of MOG_{35-55} or NFM_{15-35} (1 mg/mL) in CFA containing a final concentration of 0.5 mg/mL heat-killed *Mycobacterium tuberculosis* (H37 RA *Mtb*) in Incomplete Freund's Adjuvant (BD). Draining lymph nodes were harvested 12-14 days after priming. Single cell

suspensions were generated by passing cells through a 100μm cell strainer and directly assessed for antigen specific proliferation by uptake of [^{3}H] tritiated thymidine (VWR International, Inc). 6×10^5 primed lymph node cells or naïve 2D2 splenocytes were cultured in a 96-well flat bottom plate with indicated peptides and concentrations. After 48 hours, ^{3}H-thymidine (0.4μCi/well) was added to the culture media for 24 hours before the cells were harvested onto a filtermats (PerkinElmer) with the FilterMate 196 harvester (Packard). ^{3}H-thymidine uptake was analyzed with the 1450 Microbeta TriLux microplate liquid scintillation counter (PerkinElmer). Cell culture media contained RPMI 1640 (CellGro) supplemented with 10% heat-inactivated FBS (Gibco-Life Technologies), 4mM L-glutamine (CellGro), 0.01M HEPES (CellGro), 100μg/mL gentamicin (CellGro), 20μM 2-ME (Sigma-Aldrich). Stimulation index was calculated as a ratio of the counts per minute between peptide stimulated versus unstimulated cells.

Induction of EAE

EAE was induced with two subcutaneous injections of emulsion delivering 200μg designated peptide and 0.4mg *Mtb* in IFA per injection on days 0 and 7. 250ng of pertussis toxin (List Biologicals) was concomitantly administered intraperitoneally to mice on days 0 and 2. Mice were monitored for signs of disease including weight loss and paralytic symptoms. Mice presented with typical ascending paralysis scored accordingly; (0.5) partial tail paralysis, (1.0) complete tail paralysis, (2.0) hindlimb weakness, (2.5) ataxia, (3.0) partial hindlimb paralysis, (3.5) complete hindlimb paralysis, (4.0) inability to right itself, and (5.0) moribund.

Passive EAE was generated by adoptive transfer of 1×10^7 cells from an NFM T cell line per C57BL/6 mouse, irradiated with 400rads one day before transfer. The T cell line was generated by inducing either wild type C57BL/6 mice (naturally Thy1.2) or Thy1.1 congenic C57BL/6 mice with $NFM_{15\text{-}35}$ in CFA on days 0 and 7 with pertussis toxin administered on days 0 and 2 as described above. Spleens were harvested 14 days later, mashed into single cell suspensions and cultured as previously described but with the addition of 50 ng/ml of IL-2 and 5ng/mL recombinant mouse IL-12 (Gemini Bio). Splenocytes were cultured for 3 days and with 10×10^6 blast cells transferred intraperitoneally (i.p.). Mice were then monitored for signs of EAE.

Antibody characterization of T cells enriched by tetramer pulldown

Tetramer enrichment was performed as previously described (32). In brief, spleen and peripheral lymph nodes (inguinal, lumbar, mesenteric, cervical, axillary and brachial) were harvested and processed into a single cell suspension by passing through a 100μm strainer. Cells were washed in cold 1X HBSS (Cellgro) and resuspended with 4μg/mL of tetramer PE conjugated NFM:I-A^b and/or APC conjugated MOG:I-A^b (NIH tetramer core (33, 34)) in Fc block (heat killed mouse and rat serum, Sigma-Aldrich) at a volume 2× the pellet volume. After 1hr at room temperature, cells were wash in cold FACS wash (0.1% BSA, 0.05% NaN3, 1x PBS) and resuspend in 200μL FACS wash plus 50μL of anti-PE and/or anti-APC beads (Miltenyi Biotec) and incubated for 30 min. on ice. Cells were then washed and enriched on a LS column (Miltenyi Biotec). Unbound and column bound cell numbers were determined with AccuCheck microbeads (Invitrogen) alongside with cell surface marker

characterization performed with flow cytometry (LSR II, BD) and FlowJo software (Treestar). Antibodies used included; CD3ε-FITC (145-2C11, BD Pharmingen), CD11b-PerCP -Cy5.5 (M1/70, BD Pharmingen), CD11c-PerCP-Cy5.5 (HL3, BD Pharmingen), CD19- PerCP -Cy5.5 (1D3, Tonbo Biosciences), CD4-Brilliant Violet 510 (RM4-5, BioLegend), CD8-Brilliant Violet 785 (53-6.7, BioLegend), CD44-Alexa Fluor 700 (IM7, eBioscience).

T cell isolation from CNS

Mice were euthanized by CO_2 induced asphyxiation and perfused with 1X Dulbecco's PBS (CellGro) through the left ventricle with drainage mediated by laceration of the inferior vena cava. From individual mice, single cell suspensions of the CNS, brain and spinal cord, were generated by passing the tissue through a 100μm strainer. Mononuclear cells were isolated by Percoll density centrifugation (Sigma-Aldrich). $CD4^+$ T cells were isolated from pooled CNS mononuclear cells using MACS with L3T4 CD4 positive selecting beads (Miltenyi Biotec). Enriched T cells were assessed for antigen specificity and effective 2D affinities using the 2D micropipette adhesion frequency assay using pMHC coated RBC sensors (25, 27, 35-37).

2D micropipette adhesion frequency assay and analysis

Human RBCs were isolated from healthy volunteers in accordance with the Institutional Review Board at Emory University. RBCs were prepared by first coating the cells with varying concentrations of Biotin-X-NHS (EMD Millipore) followed by 0.5mg/mL streptavidin (ThermoFisher Scientific) and then 1μg of biotinylated monomers MOG_{38-49}:I-A^b, NFM_{18-30}:I-A^b, GP_{66-77}:I-A^b (NIH Tetramer Core Facility). Quantitation of TCR and pMHC densities were determined by flow cytometry (LSR II, BD) after labeling with PE conjugated TCRβ (H57-597, eBioscience) or I-A/I-E (M5/114.15.2, BD) and quantitated with PE-Quantibrite bead standards (BD).

Adhesion frequencies between T cells and pMHC RBC sensors were determined if binding, visualized by RBC membrane distension, was observed after individual T cells were brought into contact 25-50 times with movement controlled by a piezo actuator (38). Background or non-specific adhesion frequencies are considered to be below 0.1 in this antigen specific system (25). Adhesion frequencies along with molecule surface densities were used to calculate effective 2D affinities (A_cK_a) using $A_cK_a = -\ln[1-P_a(\infty)]/m_rm_l$ with m_r and m_l representing TCR and pMHC surface densities, respectively.

Testing individual T cells among multiple pMHC is done by sequential binding. First, RBC sensors with different pMHC are concentrated at opposing locations within the microscope chamber containing purified T cells. Next, one T cell is aspirated into the micropipette attached to the piezo actuator and the MOG_{38-49}:I-A^b RBC sensor is aspirated into the second micropipette. After 25-50 touches the MOG RBC sensor is expelled and then the NFM_{18-30}:I-A^b RBC sensor can be aspirated and tested against the same aspirated T cell. The next individual T cell will be tested in reverse order from the previous assessment, i.e. the NFM sensor first followed by the MOG sensor in order to assess if the sequential order influences subsequent antigen binding.

Statistics

Statistical analyses were performed with Prism version 6 (GraphPad Software). Disease onset was assessed by unpaired, nonparametric t tests with Mann-Whitney post hoc tests. Two-tailed unpaired parametric t tests with F test variances were used for analyses between 2 groups while comparison of multiple means were performed with one-way ANOVA. Paired t tests were run where single cell detection of MOG versus NFM specificity was directly compared.

Results

NFM$^{-/-}$ mice reveal MOG$_{35-55}$ is the primary encephalitogenic antigen

The experiments highlighted here are aimed at clarifying the encephalitogenic potential of NFM based on the work initially describing T cell cross-reactivity between MOG$_{35-55}$ and NFM$_{15-35}$ in polyclonal MOG and NFM cell lines (14). We also found both MOG$_{35-55}$ and NFM$_{15-35}$ to be immunogens based on proliferation of polyclonal lymph node cells directly *ex vivo* using a range of peptide doses to determine sensitivity of the T cell response, Fig. 1A. Restimulation of lymph node cells with the cognate priming antigen revealed that higher peptide concentrations (10μM to 100μM) were needed to see proliferation above background. Interestingly, cross-reactive proliferation to the non-cognate antigen was poorly detected, if at all, despite 6 of the 9 putative core epitopes being identical between NFM$_{20-28}$ and MOG$_{40-48}$. This indicated that T cell expansion via the cross-reactive, non-cognate epitope was not significant on the polyclonal level, questioning the relevance of cross-reactive expansion to disease. C57BL/6 mice actively challenged with NFM$_{15-35}$ using a conventional induction regimen lacked the weight loss and encephalitogenic potential exhibited by MOG$_{35-55}$, Fig. 1B (14, 28).

To more clearly tease apart the contribution of NFM$_{15-35}$ to the polyclonal response, we used mice deficient in NFM (NFM$^{-/-}$) (30). Agouti mice double deficient in NFM and NFH proteins were generously obtained from Dr. Julien and subsequently backcrossed in our laboratory with our progeny confirmed as NFM$^{-/-}$, NFH$^{+/+}$ and 99% C57BL/6N by speed congenics (DartMouse, Fig. 2A), PCR (Fig. 2B) and histology (Fig. 2C). NFM deficient mice were used to eliminate potential thymic and peripheral selection pressures due to the expression of NFM by medullary and cortical thymic epithelial cells (39, 40). NFM$_{15-35}$ primed lymph node cells from wild type or NFM deficient mice gave a similar *ex vivo* proliferative response between the mice, Fig. 2D. This showed that NFM$_{15-35}$ was equally immunogenic regardless of NFM expression. The course of MOG induced EAE was then characterized in the NFM deficient mice in order to eliminate potential T cell cross-reactivity with NFM. We hypothesized that if T cell cross-reactivity to NFM contributed to EAE onset or severity then a diminished disease course would be seen in the absence of NFM. NFM$^{-/-}$ mice however developed EAE similarly to wild type NFM sufficient mice with no difference in day of symptom onset and overall disease course, Fig. 2E. Furthermore, NFM$_{15-35}$ challenge was unable to induce EAE in MOG$^{-/-}$ mice clearly indicating that NFM alone is not sufficient to cause EAE, Fig. 2F.

Tetramer positive, MOG specific T cells expand poorly after NFM_{15-35} priming

The absence of NFM induced EAE was similar to our previously published reports with the MOG 45D variant peptide, which like NFM shares all primary TCR contact residues with wild type MOG but differs at MHC anchor residues (33, 41). Interestingly, MOG 45D could induce EAE and expand MOG_{38-49} specific, tetramer positive T cell when IFNγ signaling was deficient in mice (33). We therefore tested whether NFM_{15-35} challenge of $IFN\gamma R^{-/-}$ would induce EAE and found NFM_{15-35} was still not encephalitogenic, Fig. 3A. Since the MOG 45D data suggested a threshold level of MOG tetramer positive T cells was needed for onset of polyclonal EAE, we monitored antigen specific T cell expansion in C57BL/6 mice after MOG_{35-55} or NFM_{15-35} to assess why NFM_{15-35} challenge does not induce EAE.

Cell numbers of tetramer positive T cells were examined at days 14 and 22 post challenge with MOG_{35-55} and NFM_{15-35}, days typical of onset and peak paralytic symptoms in our laboratory (33, 41-43) using the tetramer pulldown technique to enhance detection and quantitation of T cells within the polyclonal repertoire (32), Fig. 3. At day 14 after MOG_{35-55} challenge, the MOG specific T cell population expanded to 16,000 cells ± 2,200 (mean ± SEM) with only a subtle decline in numbers to 9,200 cells ± 1,800 by day 22 ($p=0.02$, Fig. 3B). NFM_{15-35} challenge maximally expanded cross-reactive MOG_{38-49} specific T cells to a number 5-times lower than MOG_{35-55} challenge at day 14, respectively 3,200 cells ± 770 which further diminished 34% by day 22 to 1,100 cells ± 410, $p=0.018$. Breakdown of the day 22 MOG_{38-49} tetramer positive populations into $CD4^+$ $CD44^{hi}$ versus $CD4^+$ $CD44^{low}$ indicated how well T cells were being activated by the antigen priming regimen, Fig. 3C. MOG_{35-55} challenge significantly expanded a greater number of $CD44^{hi}$ (9,200 cells ± 1,800) than $CD44^{low}$ cells (1,360 cells ± 290), while NFM priming did not with 1,100 cells ± 410 versus 4,300 cells ± 2,000 respectively.

We considered that endogenous NFM expression could potentially regulate the expansion of MOG_{38-49} tetramer positive T cells after NFM_{15-35} challenge. We used the tetramer pulldown method to enumerate any changes in T cell expansion between NFM deficient and wild type mice 22 days post challenge. We found a similar expansion ($p=0.41$) of MOG_{38-49} specific T cells after NFM_{15-35} challenge between wild type C57BL/6 mice (1,500 cells ± 580) and NFM-/- mice (890 cells ± 460), Fig. 3D suggesting that endogenous expression of NFM was not negatively regulating expansion of MOG_{38-49} tetramer positive cells in peripheral spleen and lymph nodes at this time point.

The identification of polyclonal NFM_{18-30} specific T cells in the spleen and lymph nodes was difficult without enriching for the cells by tetramer pulldown. Low level detection was possible with this method, most notably at day 14 post challenge, Fig. 3E & F. There was no significant difference in the detection of NFM_{18-30} tetramer positive cells between MOG_{35-55} versus NFM_{15-35} challenge at days 14 (respectively 6,100 cells ± 1,000 and 3,500 cells ± 980, $p=0.09$) and 22 ($p=0.25$ at 1,400 cells ± 490 and 760 cells ± 210 respectively). Yet NFM_{18-30} specific T cells numbers were significantly diminished by day 22 when compared to the numbers seen at day 14 following MOG_{35-55} challenge ($p=0.0004$) and NFM_{15-35} challenge ($p=0.008$).

The notable difference in peripheral detection of MOG_{38-49} T cells identified 22 days after NFM_{15-35} challenge, Fig. 3B, spurred the question whether the missing peripheral MOG specific T cells had migrated to the CNS by this time point, Fig. 3G. $CD4^+$ $CD44^{hi}$ MOG_{38-49} specific T cells were found in the CNS after MOG_{35-55} (760 cells ± 240) but not NFM_{15-35} challenge (2.7 cells ± 1.7) despite a similar number of $CD3^+$ $CD4^+$ $CD44^{hi}$ T cell infiltrates (25,000 cells ± 7,200 and 9,800 cells ± 3,000 respectively). There was limited detection of tetramer positive NFM_{18-30} specific T cells after MOG_{35-55} challenge (32.8 cells ± 7.0) with no detection of this population in the CNS following NFM_{15-35} challenge (2.2 cells ± 1.5). The antigen specificity of the remaining $CD3^+$ infiltrates could not be determined by MOG_{38-49} and NFM_{18-30} tetramer.

N-terminal alterations in the NFM peptide restore encephalitogenicity and highlight residues critical for expansion of cross-reactive, tetramer positive, MOG specific T cells

The poor expansion and sustainability of cross-reactive, MOG_{38-49} specific T cells after NFM_{15-35} challenge allowed us to probe which amino acids within the NFM_{20-28} core nonamer would expand encephalitogenic T cells that cross recognized MOG_{38-49}. Published data indicated NFM poorly binds $I\text{-}A^b$, therefore we first modified NFM_{20-28} at proposed MHC anchor residues (positions P1, P4, and P9 within the NFM_{20-28} core) and tested their ability to promote EAE. The P6 anchor residue was not modified because serine is found at this position in both MOG_{35-55} and NFM_{15-35} peptides. The NFM specific amino acids were swapped with the respective residues found within MOG_{35-55}, Table I. P1 (40Y) of MOG_{35-55} is a critical MHC anchor residue shown by $I\text{-}A^b$ peptide-competition assays such that, functionally, an alanine substitution at this position results in a loss of MOG specific T cell responsiveness (42, 44-46). We therefore made NFM variant T20Y at P1, challenged mice and found that encephalitogenic potential increased 33% incidence in comparison to the complete absence of disease compared to wild type NFM_{15-35} challenge (Fig. 4A and Table II) confirming a previously reported (40). We generated additional NFM_{15-35} MHC variant peptides at P4 and P9 to have the MHC anchor residues of the MOG_{40-48} nonamer, respectively S23P and S28V, but these peptides did not promote EAE Fig. 4A. The suboptimal induction of disease with the P1 change alone suggested that P1 along with residues outside of the core nonamer may be important for inducing 100% incidence of EAE.

Published data shows that $I\text{-}A^b$ can tolerate changes in the peptide MHC anchor positions through predicted hydrogen bonding with peptide N-terminal residues at P-1 and -2 (45) and that alanine substitutions at P-1 reduce proliferation of MOG specific T cell lines (44). We subsequently engineered NFM_{15-35} with the amino acids found at MOG_{35-55} P-1 concomitantly with the T20Y mutation at P1generating the double mutant NFM E19W, T20Y (Table I). Introduction of aromatic side chains at P-1 and P1 restored encephalitogenicity to 100% incidence compared to NFM_{15-35} (Fig. 4B & Table II). The 2D2 TCR transgenic model used to initially define MOG and NFM cross-reactivity showed the dose response curve for NFM E19W, T20Y to be most similar to MOG_{35-55}, exhibiting maximal proliferation at 10μM peptide. The NFM T20Y proliferative response was most similar to NFM_{15-35} and marked by maximal proliferation at 1μM peptide, Fig. 4C. This reiterates the importance of W at P-1 for the characteristic MOG responsiveness.

We appreciated that the N terminal substitutions were influencing polyclonal encephalitogenicity as well as MOG versus NFM responsiveness in 2D2 T cells and wanted to further clarify how these substitutions affected expansion of MOG_{38-49} and NFM_{18-30} tetramer positive cells within the polyclonal EAE response, Fig. 4D. High affinity, MOG_{38-49} tetramer positive cells expanded similarly (p=0.45) between NFM E19W, T20Y (7,300 cells ± 1,400) and wild type MOG_{35-55} induced EAE (9,200 cells ± 1,800), Fig. 4D left panel. Expansion of MOG_{38-49} specific T cells was significantly reduced after challenge with NFM variant T20Y (2,000 cells ± 540) or wild type NFM_{15-35} (1,100 cells ± 410) when compared to the numbers expanded by MOG_{35-55} (p=0.006 and p<0.0001 respectively) or NFM E19W, T20Y (p=0.003 and p<0.0001 respectively). There was no significant difference between expansion of MOG_{38-49} specific T cells by T20Y and NFM_{15-35}, p=0.244, which could relate to inconsistent EAE onset with this antigen. Detection of NFM_{18-30} specific T cells by tetramer was not enhanced by any amino acid substitution examined with no significant difference among the groups p=0.68, Fig. 4D right panel. Overall, the encephalitogenicity of NFM variant peptides was dependent on expansion of higher affinity, MOG_{38-49} tetramer positive T cells and not NFM_{18-30} specific T cells.

Polyclonal NFM specific T cells are predominantly cross-reactive to MOG during the course of MOG_{35-55} induced EAE as assessed by the 2D micropipette adhesion frequency assay

We previously reported that MOG tetramer enriches for high affinity T cells, so reduced detection of higher affinity, NFM_{18-30} specific T cells by tetramer suggested that these T cells display TCR with generally low affinity or avidity interactions with pMHC (25). The 2D micropipette adhesion frequency assay provides a more sensitive technology to sample antigen specificity and effective 2D affinity interactions among individual T cells within the polyclonal response without using avidity based tetramers. We previously reported that tetramer poorly detected MOG_{38-49} : $I\text{-}A^b$ or MOG_{42-55} : $I\text{-}A^{g7}$ specific T cells when compared to the 2D micropipette adhesion frequency assay (25, 26). Similarly, tetramer also underestimated the percent detection of NFM_{18-30} : $I\text{-}A^b$ specific T cells ~100 times less when compared to detection by the 2D micropipette adhesion frequency assay, respectively 0.5% versus 55% Fig. 5A. NFM_{18-30}:$I\text{-}A^b$ monomeric detection of T cells was specific as demonstrated by lack of binding to $CD4^+$ SMARTA T cells, specific for LCMV glycoprotein epitope 61-80, Fig. 5B.

$CD4^+$ T cells isolated from the CNS were monitored by the 2D micropipette adhesion frequency assay for MOG_{38-49} and NFM_{18-30} specificity and affinity throughout the course of MOG_{35-55} induced EAE in C57BL/6 mice, particularly at onset of paralytic symptoms (days 12-16 post MOG_{35-55} induction), peak (days 20-23 post induction) and more chronic time points (days 28-32 post induction), Fig. 5C. NFM_{18-30}: $I\text{-}A^b$ and MOG_{38-49}: $I\text{-}A^b$ RBC sensors were placed at opposing ends of the media chamber, to prevent mixing, and individual T cells were tested in random sequence with the sensors. This means one cell was tested for MOG_{38-49} specificity first followed by NFM_{18-30} assessment while the second T cell was tested in the opposite order to rule out potential biasing of TCR:pMHC recognition based on memory of a previous pMHC (47). The order of TCR contact with MOG or NFM pMHC did not alter the overall adhesion frequency (Supplementary Figure 1). Geometric

mean affinities of MOG_{38-49} specific T cells at onset, peak and chronic time points are reported as 1.1×10^{-5} μm^4, 6.2×10^{-6} μm^4 and 1.1×10^{-5} μm^4 respectively. NFM_{18-30} specific T cells exhibited means of 1.4×10^{-5} μm^4 at onset, 1.1×10^{-5} μm^4 at peak and 9.5×10^{-6} μm^4 at chronic time points. Unpaired parametric t-test comparisons of the mean MOG and NFM affinities per time point indicated no significant differences between the groups assuming equal standard deviations ($p\geq0.058$).

Although the means were similar, the breadth of affinities seen within the MOG_{38-49} specific population differed from NFM_{18-30} specific cells, Fig. 5C. Significant differences in affinity ranges between these two populations were seen at onset ($F(52,30)=2.7$, $p=0.004$) and chronic ($F(48,36)=2.0$, $p=0.029$) time points as measured by the F-test to compare variances. The greatest breadth in maximal / minimal 2D affinities were seen at onset with breadths of 1,927 for MOG_{38-49} : I-A^b and 158 for NFM_{18-30} : I-A^b, a finding we also reported during EAE onset in NOD mice (26). NFM_{18-30} specific T cells with high 2D affinities were absent from detection at peak and chronic time points using 1.1×10^{-4} μm^4 as a cutoff for high affinity previously published for MOG_{38-49} : I-A^b T cells (25). At onset, the few high affinity NFM_{18-30} specific T cells found remained close to this cutoff with a geometric mean of 1.3×10^{-4} μm^4, an affinity below the MOG_{38-49} specific population at 6.1×10^{-4} μm^4. Overall, there is a deficit in the number of higher affinity NFM specific T cells detected by both the 2D micropipette adhesion frequency assay and tetramer, Fig. 3.

The total percentage of cells that recognize MOG_{38-49} versus NFM_{18-30} on average (SD) is not significantly different at onset, peak or chronic time points $p \geq 0.1864$, Fig. 5D. This suggested that there was significant T cell cross-recognition between MOG and NFM. Analysis of individual T cells from the CNS indicated that each cell has a unique, intrinsic capacity to cross-recognize MOG_{38-49} and NFM_{18-30}. Importantly, individual T cells tested against multiple pMHC revealed that TCR affinity for one antigen did not dictate strength of recognition to the second antigen, meaning high affinity for MOG does not indicate high affinity for NFM or vice versa, Fig. 5E. Breakdown of single cell cross-recognition, Fig. 5F, indicated that among all time points it was rare to find T cells in the CNS that recognized NFM_{18-30} only and not also MOG_{38-49}, occurring at 5.7% to 11.3% of the population. The majority of T cells in the CNS at peak (58.6%) or chronic (56.6%) disease actually recognized both MOG_{38-49} and NFM_{18-30}, denoted as double binders. Therefore, the NFM_{18-30} specific T cells at peak and chronic time points are predominantly MOG_{38-49} specific at 91.1% and 83.3% respectively. One should note that the NFM only T cells could be functionally MOG reactive but below the limit of detection by the 2D micropipette adhesion frequency assay, a phenotype exhibited by 2D2 T cells (34). At onset (Fig. 5E) it was rare to find T cells displaying a 2D2-like phenotype of measurable affinity for NFM and not MOG, only 4 of the 56 cells tested at onset. Overall, 12 of the 56 T cells displayed heteroclitic affinities for NFM over MOG compared to 26 of the 56 cells displaying affinities dominant for MOG over NFM.

The dominant cross-reactivity of NFM specific cells with MOG led us to track MOG specificity in a NFM T cell line previously reported to promote EAE (14). Krishnamoorthy, *et al.* showed a NFM line could proliferate to both MOG and NFM and we confirm this cross-recognition with the 2D micropipette adhesion frequency assay, Fig. 6A. A Thy1.1$^+$

NFM_{15-35} T cell line was adoptively transferred into irradiated C56BL/6 $Thy1.2^+$ recipients with no additional administration of CFA, peptide antigen or pertussis toxin. After EAE onset (Fig. 6B), we tested antigen specificity of the CNS infiltrates and found MOG_{38-49} but not NFM_{18-30} tetramer positive cells present in the CNS, Fig. 6C. The CNS cell population was a mix of Thy1.1 positive and negative cells with the Thy1.1 NFM cell line being the source of the $CD44^{hi}$ MOG tetramer positive T cells, Fig. 6D. NFM_{18-30} specific T cell contributions to EAE are strongly associated with MOG_{38-49} specific cross-recognition and not stand alone NFM reactivity. These data in total point to MOG_{35-55} as the dominant autoantigen for polyclonal T cell mediated EAE in C57BL/6 mice even when heteroclitic responsiveness to NFM is present.

Discussion

Given the identical TCR contact residues of NFM_{15-35} and MOG_{35-55}, it was surprising that NFM does not induce EAE (Fig. 1). Antigen specific T cell recognition is critical for generating a robust immune response where increased cell numbers influence the onset and magnitude of the response (48, 49). The idea that autoreactive T cell expansion is influenced by TCR cross-recognition and reactivity to peptides with alterations at TCR or MHC residues introduced through amino acid substitutions has been well documented, particularly in multiple sclerosis and EAE research (5, 15, 19, 42, 50-53). In one example, expansion of tetramer positive MOG specific T cells in the polyclonal repertoire has been reported in mice challenged with foreign derived peptides that are structurally similar to MOG_{40-48} (19). These mice developed EAE with varying degrees of severity and the weaker disease courses were associated with slightly diminished expansion of higher affinity, MOG tetramer positive T cells (19). In the case of NFM_{15-35} challenge there were reduced numbers of $CD44^{hi}$ MOG_{38-49} tetramer positive T cells in the spleen and peripheral lymph nodes which were not sustained long term when compared to MOG_{35-55} challenge (Fig. 3). Expansion of a reduced number of MOG specific cells ultimately failed to promote T cell enrichment in the CNS and EAE after NFM_{15-35} challenge (Figures 1, 3 & 4).

Important differences between the core nonamers of NFM_{15-35} and MOG_{35-55} that influence T cell reactivity are the amino acid residues proposed to interface with $I\text{-}A^b$ molecule. In fact, replacement of the P1 MHC anchor residue partially restored the disease potential of the NFM peptide. We previously reported that a MHC variant peptide of MOG_{35-55} at peptide position P6, MOG 45D, also resulted in poor encephalitogenic potential despite sharing 5 TCR contact residues with MOG_{35-55} (33). Of interest was the finding that IFNγ deficient signaling rendered mice permissive to 45D mediated EAE and that disease was concomitant with enhanced detection of MOG_{38-49} specific tetramer positive T cells. These data suggested that a threshold of high affinity, MOG_{38-49} tetramer positive T cells was needed for polyclonal T cells to establish EAE in the IFNγ deficient mice. Since IFNγ deficiency did not restore encephalitogenic potential of NFM_{15-35} as it did for 45D (Fig. 3), we addressed the role of additional amino acid differences between NFM_{15-35} and MOG_{35-55} that hindered T cell encephalitogenicity.

We found that amino acid substitutions within NFM_{15-35} enabled us to map the residues critical for encephalitogenicity and expansion of MOG_{38-49} tetramer positive T cells in a

polyclonal setting (Fig. 4). For MOG_{35-55}, evidence suggested that amino acid residues P-1 and P-2 outside of the core nonamer contribute to MHC anchoring and to TCR binding in individual clones (44, 45, 54, 55) with implications for T cell recognition of NFM_{15-35} (28). We focused on modulating NFM at P1 (T20Y) to mirror MOG at that position because Petersen *et al.* reported that MOG Y40 was important for MHC binding and T cell responsiveness (44); S23P and S28V MHC anchor substitutions were tested in comparison. S23P and S28V did not promote EAE in C57BL/6 mice and T20Y exhibited a low incidence of disease (Table II), a phenotype published during this time (40). We further showed that dual alterations at NFM_{15-35} P-1 (E19W) and P1 (T20Y) enhanced EAE incidence to 100%, Table II. It was interesting that EAE incidence of NFM E19W, T20Y was concomitant with expansion of polyclonal MOG_{38-49} tetramer positive T cells and a MOG-like proliferation profile by 2D2 monoclonal T cells (Fig. 4). Expansion of high numbers of polyclonal MOG_{38-49} tetramer positive T cells was clearly dependent on the Y20 and W19 amino acids at P1 and P-1 respectively. Mapping of the amino acids required for expansion of tetramer positive T cells suggested that a threshold number of MOG_{38-49} specific T cells was required for consistent onset of disease, namely an average of 7,324 to 9,244 cells seen with NFM E19W, T20Y and MOG_{35-55}.

NFM deficient mice were used to indicate whether antigen specific selection pressures influenced encephalitogenicity. Although it was possible that T cells educated in these mice would be hyperresponsive to NFM based on reports showing enhanced antigen specific T cell responses in $MBP^{-/-}$ and $MOG^{-/-}$ mice (29, 56), we saw no significant difference in NFM specific T cell proliferation between wild type and NFM deficient mice (Fig. 2). This could likely relate to the findings that peptides with low affinity for MHC do not mediate thymocyte negative selection, which first came to prominence with acetylated MBP (57). Our group also found this true for a model antigen system (58). It is not totally unexpected that deletion failed to alter the NFM specific T cell response considering the MHC alterations inherent in NFM $_{15-35}$ elicit a weaker association for $I\text{-}A^b$ than MOG_{35-55} (28), which is consistent with the high concentration of NFM required to tolerize EAE compared to MOG (59). In support of this, our studies revealed that cross-reactivity was not altered between wild type and $NFM^{-/-}$ mice because MOG_{35-55} induced EAE similarly in both mouse strains (Fig. 2). Furthermore, a report published during this time showed that *ex vivo* T cell cross-reactivity between MOG and NFM could be enhanced in $MOG^{-/-}$ but not $NFM^{-/-}$ mice (40). These data combined with the finding that NFM_{15-35} challenge of $MOG^{-/-}$ mice still did not induce EAE through cross-reactivity (Fig. 2) supported the finding that NFM is not a critical T cell antigen in polyclonal EAE.

The equivalent disease severity exhibited by our $NFM^{-/-}$ mice after MOG_{35-55} challenge differed somewhat from another report showing reduced EAE severity in the absence of NFM (59). Our mice (30) backcrossed to C57BL/6N had fulminant EAE and it is not known whether environmental or genetic factors caused this point of phenotypic divergence. However, our data still supports the observations of Ramadan *et al.* that NFM expression was not required for T cell mediated EAE (59). This is consistent with the reports that proliferation and cytokine production by MOG specific T cells were markedly diminished by restimulation with NFM compared to cognate MOG (28, 40, 59). We support that CNS T cell infiltrates are functionally responsive to NFM during EAE (14, 28), because pMHC

monomers detected T cell cross-recognition of MOG_{38-49} and NFM_{18-30} by the majority of infiltrates at peak and chronic time points (Fig. 5).

Dissecting the role of individual cross-reactive clones in EAE lends to observations of heteroclitic responses where there is enhanced recognition and responsiveness to a second epitope above the initial priming antigen (Fig. 5). Heteroclitic behavior is best documented with clonal TCR in response to peptides with amino acid substitutions at TCR or MHC contacts but how one clone reflects on the bulk polyclonal response is less clear and dependent on previous antigenic exposures (12, 57, 60-62). Furthermore the priming antigen whether NFM_{15-35} or MOG_{35-55} could lead to asymmetry or skewedness of the immune response based on divergent expansion of unique T cell clones. Certainly there are reported differences in percentage detection of individual TCRα and TCRβ usage after priming with these respective peptides (14), yet overlap exists with divergence being dictated by a few amino acids at P1 and P-1 at the N-terminus of the core nonamer, Fig. 4. The sequence similarities between MOG_{35-55} and NFM_{15-35} and the current data in the field support that T cells are largely bispecific between these two peptides. We would argue that our analyses question the functional significance of NFM_{15-35} on a polyclonal level because NFM monospecific T cells are rare in the population, Fig.5. Even in the presence of heteroclitic recognition of NFM, we found MOG to be the dominant autoantigen for disease onset in the absence of stand-alone encephalitogenicity by NFM_{15-35} (Fig. 2).

The expansion of high affinity, MOG tetramer positive T cells are a relatively small population within the polyclonal repertoire (25-27, 63) and expansion or engraftment numbers has been associated with spontaneous EAE in retrogenic models (49). While NFM can expand a limited number of MOG tetramer positive T cells, these cells are not able to migrate to the CNS and cause EAE. We would argue that NFM is not providing a strong enough stimulus to evoke de novo EAE based on the weak interaction with $I\text{-}A^b$, which can be overcome with amino acid substitutions (Fig. 4). Culturing NFM primed splenocytes with NFM was a means to enhance T cell recognition and activation on NFM to enhance expansion encephalitogenic NFM or MOG specific T cell clones (14, 64, 65). As previously reported, NFM expanded T cells were able to passively transfer EAE, but we found this was associated with transfer of cross-reactive MOG_{38-49} tetramer positive T cells capable of enrichment in the CNS (Fig. 6). This again showcased NFM without stand-alone encephalitogenic potential and supported MOG as the critical determinant in the bispecific model required for onset of demyelinating autoimmune disease. Overall, our experiments here indicate that expansion of a threshold number of high affinity, MOG tetramer positive T cells within the polyclonal response is a readout of encephalitogenic potential.

Supplementary Material

Refer to Web version on PubMed Central for supplementary material.

Acknowledgments

We acknowledge the NIH Tetramer Core Facility at Emory University for providing pMHC tetramers and biotinylated pMHC monomers for use in the tetramer pulldown and 2D micropipette adhesion frequency assays. We thank Dr. Marla Gearing from the Emory NINDS Neuropathology / Histochemistry Core Facility for her

collaborative spirit and helpful comments on presenting the histological data. We also thank Jennifer Cosby for additionally reviewing the manuscript.

This research was supported with funding from the National Institutes of Health (NIH) and the National Multiple Sclerosis Society (NMSS). BE R01 grants supporting this research include NS071518 (NINDS) and AI110113 (NIAID). LB was supported by a postdoctoral fellowship from the NMSS [FG1963A1/1]. JS is currently funded by the NIH (R25 NS070680) and the NMSS (127992A).

References

1. Bielekova B, Sung MH, Kadom N, Simon R, McFarland H, Martin R. Expansion and functional relevance of high-avidity myelin-specific CD4+ T cells in multiple sclerosis. J Immunol. 2004; 172:3893–3904. [PubMed: 15004197]
2. Yu W, Jiang N, Ebert PJ, Kidd BA, Muller S, Lund PJ, Juang J, Adachi K, Tse T, Birnbaum ME, Newell EW, Wilson DM, Grotenbreg GM, Valitutti S, Quake SR, Davis MM. Clonal Deletion Prunes but Does Not Eliminate Self-Specific alphabeta CD8(+) T Lymphocytes. Immunity. 2015; 42:929–941. [PubMed: 25992863]
3. Kieback E, Hilgenberg E, Stervbo U, Lampropoulou V, Shen P, Bunse M, Jaimes Y, Boudinot P, Radbruch A, Klemm U, Kuhl AA, Liblau R, Hoevelmeyer N, Anderton SM, Uckert W, Fillatreau S. Thymus-Derived Regulatory T Cells Are Positively Selected on Natural Self-Antigen through Cognate Interactions of High Functional Avidity. Immunity. 2016; 44:1114–1126. [PubMed: 27192577]
4. Isobe NL, Madireddy P, Khankhanian T, Matsushita SJ, Caillier JM, More PA, Gourraud JL, McCauley AH, Beecham C, International Multiple Sclerosis Genetics. Piccio L, Herbert J, Khan O, Cohen J, Stone L, Santaniello A, Cree BA, Onengut-Gumuscu S, Rich SS, Hauser SL, Sawcer S, Oksenberg JR. An ImmunoChip study of multiple sclerosis risk in African Americans. Brain. 2015; 138:1518–1530. [PubMed: 25818868]
5. Su LF, Kidd BA, Han A, Kotzin JJ, Davis MM. Virus-specific CD4(+) memory-phenotype T cells are abundant in unexposed adults. Immunity. 2013; 38:373–383. [PubMed: 23395677]
6. Korn T, Kallies A. T cell responses in the central nervous system. Nat Rev Immunol. 2017; 17:179–194. [PubMed: 28138136]
7. Trowsdale J. The MHC, disease and selection. Immunol Lett. 2011; 137:1–8. [PubMed: 21262263]
8. Riedhammer C, Weissert R. Antigen Presentation, Autoantigens, and Immune Regulation in Multiple Sclerosis and Other Autoimmune Diseases. Front Immunol. 2015; 6:322. [PubMed: 26136751]
9. Schubert DA, Gordo S, Sabatino JJ Jr, Vardhana S, Gagnon E, Sethi DK, Seth NP, Choudhuri K, Reijonen H, Nepom GT, Evavold BD, Dustin ML, Wucherpfennig KW. Self-reactive human CD4 T cell clones form unusual immunological synapses. J Exp Med. 2012; 209:335–352. [PubMed: 22312112]
10. Wucherpfennig KW, Strominger JL. Molecular mimicry in T cell-mediated autoimmunity: viral peptides activate human T cell clones specific for myelin basic protein. Cell. 1995; 80:695–705. [PubMed: 7534214]
11. Legoux FP, Lim JB, Cauley AW, Dikiy S, Ertelt J, Mariani TJ, Sparwasser T, Way SS, Moon JJ. CD4+ T Cell Tolerance to Tissue-Restricted Self Antigens Is Mediated by Antigen-Specific Regulatory T Cells Rather Than Deletion. Immunity. 2015; 43:896–908. [PubMed: 26572061]
12. Cole DK, Bulek AM, Dolton G, Schauenberg AJ, Szomolay B, Rittase W, Trimby A, Jothikumar P, Fuller A, Skowera A, Rossjohn J, Zhu C, Miles JJ, Peakman M, Wooldridge L, Rizkallah PJ, Sewell AK. Hotspot autoimmune T cell receptor binding underlies pathogen and insulin peptide cross-reactivity. J Clin Invest. 2016; 126:2191–2204. [PubMed: 27183389]
13. Sethi DK, Gordo S, Schubert DA, Wucherpfennig KW. Crossreactivity of a human autoimmune TCR is dominated by a single TCR loop. Nat Commun. 2013; 4:2623. [PubMed: 24136005]
14. Krishnamoorthy G, Saxena A, Mars LT, Domingues HS, Mentele R, Ben-Nun A, Lassmann H, Dornmair K, Kurschus FC, Liblau RS, Wekerle H. Myelin-specific T cells also recognize neuronal autoantigen in a transgenic mouse model of multiple sclerosis. Nat Med. 2009; 15:626–632. [PubMed: 19483694]

15. Wooldridge L, Ekeruche-Makinde J, van den Berg HA, Skowera A, Miles JJ, Tan MP, Dolton G, Clement M, Llewellyn-Lacey S, Price DA, Peakman M, Sewell AK. A single autoimmune T cell receptor recognizes more than a million different peptides. J Biol Chem. 2012; 287:1168–1177. [PubMed: 22102287]

16. Birnbaum ME, Mendoza JL, Sethi DK, Dong S, Glanville J, Dobbins J, Ozkan E, Davis MM, Wucherpfennig KW, Garcia KC. Deconstructing the peptide-MHC specificity of T cell recognition. Cell. 2014; 157:1073–1087. [PubMed: 24855945]

17. Zarnitsyna VI, Evavold BD, Schoettle LN, Blattman JN, Antia R. Estimating the diversity, completeness, and cross-reactivity of the T cell repertoire. Front Immunol. 2013; 4:485. [PubMed: 24421780]

18. Maynard J, Petersson K, Wilson DH, Adams EJ, Blondelle SE, Boulanger MJ, Wilson DB, Garcia KC. Structure of an autoimmune T cell receptor complexed with class II peptide-MHC: insights into MHC bias and antigen specificity. Immunity. 2005; 22:81–92. [PubMed: 15664161]

19. Nelson RW, Beisang D, Tubo NJ, Dileepan T, Wiesner DL, Nielsen K, Wuthrich M, Klein BS, Kotov DI, Spanier JA, Fife BT, Moon JJ, Jenkins MK. T cell receptor cross-reactivity between similar foreign and self peptides influences naive cell population size and autoimmunity. Immunity. 2015; 42:95–107. [PubMed: 25601203]

20. Evavold BD, Allen PM. Separation of IL-4 production from Th cell proliferation by an altered T cell receptor ligand. Science. 1991; 252:1308–1310. [PubMed: 1833816]

21. Sloan-Lancaster J, Evavold BD, Allen PM. Induction of T-cell anergy by altered T-cell-receptor ligand on live antigen-presenting cells. Nature. 1993; 363:156–159. [PubMed: 8483498]

22. Hsu BL, Evavold BD, Allen PM. Modulation of T cell development by an endogenous altered peptide ligand. J Exp Med. 1995; 181:805–810. [PubMed: 7836933]

23. Hong J, Persaud SP, Horvath S, Allen PM, Evavold BD, Zhu C. Force-Regulated In Situ TCR-Peptide-Bound MHC Class II Kinetics Determine Functions of CD4+ T Cells. J Immunol. 2015; 195:3557–3564. [PubMed: 26336148]

24. Liu B, Chen W, Evavold BD, Zhu C. Accumulation of dynamic catch bonds between TCR and agonist peptide-MHC triggers T cell signaling. Cell. 2014; 157:357–368. [PubMed: 24725404]

25. Sabatino JJ Jr, Huang J, Zhu C, Evavold BD. High prevalence of low affinity peptide-MHC II tetramer-negative effectors during polyclonal CD4+ T cell responses. J Exp Med. 2011; 208:81–90. [PubMed: 21220453]

26. Kersh AE, Edwards LJ, Evavold BD. Progression of relapsing-remitting demyelinating disease does not require increased TCR affinity or epitope spread. J Immunol. 2014; 193:4429–4438. [PubMed: 25267971]

27. Hood JD V, Zarnitsyna I, Zhu C, Evavold BD. Regulatory and T Effector Cells Have Overlapping Low to High Ranges in TCR Affinities for Self during Demyelinating Disease. J Immunol. 2015; 195:4162–4170. [PubMed: 26385521]

28. Lucca LE, Desbois S, Ramadan A, Ben-Nun A, Eisenstein M, Carrie N, Guery JC, Sette A, Nguyen P, Geiger TL, Mars LT, Liblau RS. Bispecificity for myelin and neuronal self-antigens is a common feature of CD4 T cells in C57BL/6 mice. J Immunol. 2014; 193:3267–3277. [PubMed: 25135834]

29. Linares D, Mana P, Goodyear M, Chow AM, Clavarino C, Huntington ND, Barnett L, Koentgen F, Tomioka R, Bernard CC, Freire-Garabal M, Reid HH. The magnitude and encephalogenic potential of autoimmune response to MOG is enhanced in MOG deficient mice. J Autoimmun. 2003; 21:339–351. [PubMed: 14624757]

30. Jacomy H, Zhu Q, Couillard-Despres S, Beaulieu JM, Julien JP. Disruption of type IV intermediate filament network in mice lacking the neurofilament medium and heavy subunits. J Neurochem. 1999; 73:972–984. [PubMed: 10461886]

31. Oxenius A, Bachmann MF, Zinkernagel RM, Hengartner H. Virus-specific MHC-class II-restricted TCR-transgenic mice: effects on humoral and cellular immune responses after viral infection. Eur J Immunol. 1998; 28:390–400. [PubMed: 9485218]

32. Moon JJ, Chu HH, Hataye J, Pagan AJ, Pepper M, McLachlan JB, Zell T, Jenkins MK. Tracking epitope-specific T cells. Nat Protoc. 2009; 4:565–581. [PubMed: 19373228]

33. Sabatino JJ Jr, Shires J, Altman JD, Ford ML, Evavold BD. Loss of IFN-gamma enables the expansion of autoreactive CD4+ T cells to induce experimental autoimmune encephalomyelitis by a nonencephalitogenic myelin variant antigen. J Immunol. 2008; 180:4451–4457. [PubMed: 18354166]
34. Rosenthal KM, Edwards LJ, Sabatino JJ Jr, Hood JD, Wasserman HA, Zhu C, Evavold BD. Low 2-dimensional CD4 T cell receptor affinity for myelin sets in motion delayed response kinetics. PLoS One. 2012; 7:e32562. [PubMed: 22412888]
35. Chesla SE, Selvaraj P, Zhu C. Measuring two-dimensional receptor-ligand binding kinetics by micropipette. Biophys J. 1998; 75:1553–1572. [PubMed: 9726957]
36. Huang J, Zarnitsyna VI, Liu B, Edwards LJ, Jiang N, Evavold BD, Zhu C. The kinetics of two-dimensional TCR and pMHC interactions determine T-cell responsiveness. Nature. 2010; 464:932–936. [PubMed: 20357766]
37. Blanchfield JL, Shorter SK, Evavold BD. Monitoring the Dynamics of T Cell Clonal Diversity Using Recombinant Peptide:MHC Technology. Front Immunol. 2013; 4:170. [PubMed: 23840195]
38. Zarnitsyna VI, Zhu C. Adhesion frequency assay for in situ kinetics analysis of cross-junctional molecular interactions at the cell-cell interface. J Vis Exp. 2011:e3519. [PubMed: 22083316]
39. St-Pierre C, Brochu S, Vanegas JR, Dumont-Lagace M, Lemieux S, Perreault C. Transcriptome sequencing of neonatal thymic epithelial cells. Sci Rep. 2013; 3:1860. [PubMed: 23681267]
40. Lucca LE, Axisa PP, Aloulou M, Perals C, Ramadan A, Rufas P, Kyewski B, Derbinski J, Fazilleau N, Mars LT, Liblau RS. Myelin oligodendrocyte glycoprotein induces incomplete tolerance of CD4+ T cells specific for both a myelin and a neuronal self-antigen in mice. Eur J Immunol. 2016
41. Wasserman HA, Beal CD, Zhang Y, Jiang N, Zhu C, Evavold BD. MHC variant peptide-mediated anergy of encephalitogenic T cells requires SHP-1. J Immunol. 2008; 181:6843–6849. [PubMed: 18981103]
42. Ford ML, Evavold BD. Regulation of polyclonal T cell responses by an MHC anchor-substituted variant of myelin oligodendrocyte glycoprotein 35-55. J Immunol. 2003; 171:1247–1254. [PubMed: 12874212]
43. Bettini M, Rosenthal K, Evavold BD. Pathogenic MOG-reactive CD8+ T cells require MOG-reactive CD4+ T cells for sustained CNS inflammation during chronic EAE. J Neuroimmunol. 2009; 213:60–68. [PubMed: 19540601]
44. Petersen TR, Bettelli E, Sidney J, Sette A, Kuchroo V, Backstrom BT. Characterization of MHC- and TCR-binding residues of the myelin oligodendrocyte glycoprotein 38-51 peptide. Eur J Immunol. 2004; 34:165–173. [PubMed: 14971042]
45. Liu X, Dai S, Crawford F, Fruge R, Marrack P, Kappler J. Alternate interactions define the binding of peptides to the MHC molecule IA(b). Proc Natl Acad Sci U S A. 2002; 99:8820–8825. [PubMed: 12084926]
46. Ben-Nun A, Mendel I, Bakimer R, Fridkis-Hareli M, Teitelbaum D, Arnon R, Sela M, Kerlero de Rosbo N. The autoimmune reactivity to myelin oligodendrocyte glycoprotein (MOG) in multiple sclerosis is potentially pathogenic: effect of copolymer 1 on MOG-induced disease. J Neurol. 1996; 243:S14–22. [PubMed: 8965116]
47. Zarnitsyna VI, Huang J, Zhang F, Chien YH, Leckband D, Zhu C. Memory in receptor-ligand-mediated cell adhesion. Proc Natl Acad Sci U S A. 2007; 104:18037–18042. [PubMed: 17991779]
48. Moon JJ, Chu HH, Pepper M, McSorley SJ, Jameson SC, Kedl RM, Jenkins MK. Naive CD4(+) T cell frequency varies for different epitopes and predicts repertoire diversity and response magnitude. Immunity. 2007; 27:203–213. [PubMed: 17707129]
49. Alli R, Nguyen P, Geiger TL. Retrogenic modeling of experimental allergic encephalomyelitis associates T cell frequency but not TCR functional affinity with pathogenicity. J Immunol. 2008; 181:136–145. [PubMed: 18566378]
50. Karin N, Mitchell DJ, Brocke S, Ling N, Steinman L. Reversal of experimental autoimmune encephalomyelitis by a soluble peptide variant of a myelin basic protein epitope: T cell receptor antagonism and reduction of interferon gamma and tumor necrosis factor alpha production. J Exp Med. 1994; 180:2227–2237. [PubMed: 7525850]

51. Nicholson LB, Greer JM, Sobel RA, Lees MB, Kuchroo VK. An altered peptide ligand mediates immune deviation and prevents autoimmune encephalomyelitis. Immunity. 1995; 3:397–405. [PubMed: 7584131]

52. Bielekova B, Goodwin B, Richert N, Cortese I, Kondo T, Afshar G, Gran B, Eaton J, Antel J, Frank JA, McFarland HF, Martin R. Encephalitogenic potential of the myelin basic protein peptide (amino acids 83-99) in multiple sclerosis: results of a phase II clinical trial with an altered peptide ligand. Nat Med. 2000; 6:1167–1175. [PubMed: 11017150]

53. Kappos L, Comi G, Panitch H, Oger J, Antel J, Conlon P, Steinman L. Induction of a non-encephalitogenic type 2 T helper-cell autoimmune response in multiple sclerosis after administration of an altered peptide ligand in a placebo-controlled, randomized phase II trial. The Altered Peptide Ligand in Relapsing MS Study Group. Nat Med. 2000; 6:1176–1182. [PubMed: 11017151]

54. Ben-Nun A, Kerlero de Rosbo N, Kaushansky N, Eisenstein M, Cohen L, Kaye JF, Mendel I. Anatomy of T cell autoimmunity to myelin oligodendrocyte glycoprotein (MOG): prime role of MOG44F in selection and control of MOG-reactive T cells in H-2b mice. Eur J Immunol. 2006; 36:478–493. [PubMed: 16453383]

55. Udyavar A, Alli R, Nguyen P, Baker L, Geiger TL. Subtle affinity-enhancing mutations in a myelin oligodendrocyte glycoprotein-specific TCR alter specificity and generate new self-reactivity. J Immunol. 2009; 182:4439–4447. [PubMed: 19299745]

56. Harrington CJ, Paez A, Hunkapiller T, Mannikko V, Brabb T, Ahearn M, Beeson C, Goverman J. Differential tolerance is induced in T cells recognizing distinct epitopes of myelin basic protein. Immunity. 1998; 8:571–580. [PubMed: 9620678]

57. Anderton SM, Radu CG, Lowrey PA, Ward ES, Wraith DC. Negative selection during the peripheral immune response to antigen. J Exp Med. 2001; 193:1–11. [PubMed: 11136816]

58. McNeil LK, Evavold BD. Dissociation of peripheral T cell responses from thymocyte negative selection by weak agonists supports a spare receptor model of T cell activation. Proc Natl Acad Sci U S A. 2002; 99:4520–4525. [PubMed: 11904393]

59. Ramadan A, Lucca LE, Carrie N, Desbois S, Axisa PP, Hayder M, Bauer J, Liblau RS, Mars LT. In situ expansion of T cells that recognize distinct self-antigens sustains autoimmunity in the CNS. Brain. 2016; 139:1433–1446. [PubMed: 27000832]

60. Petrova G, Ferrante A, Gorski J. Cross-reactivity of T cells and its role in the immune system. Crit Rev Immunol. 2012; 32:349–372. [PubMed: 23237510]

61. Nicholson LB, Waldner H, Carrizosa AM, Sette A, Collins M, Kuchroo VK. Heteroclitic proliferative responses and changes in cytokine profile induced by altered peptides: implications for autoimmunity. Proc Natl Acad Sci U S A. 1998; 95:264–269. [PubMed: 9419364]

62. Madura F, Rizkallah PJ, Holland CJ, Fuller A, Bulek A, Godkin AJ, Schauenburg AJ, Cole DK, Sewell AK. Structural basis for ineffective T-cell responses to MHC anchor residue-improved “heteroclitic” peptides. Eur J Immunol. 2015; 45:584–591. [PubMed: 25471691]

63. Martinez RJ, Andargachew R, Martinez HA, Evavold BD. Low-affinity CD4+ T cells are major responders in the primary immune response. Nat Commun. 2016; 7:13848. [PubMed: 27976744]

64. Nguyen P, Liu W, Ma J, Manirarora JN, Liu X, Cheng C, Geiger TL. Discrete TCR repertoires and CDR3 features distinguish effector and Foxp3+ regulatory T lymphocytes in myelin oligodendrocyte glycoprotein-induced experimental allergic encephalomyelitis. J Immunol. 2010; 185:3895–3904. [PubMed: 20810983]

65. Zhao Y, Nguyen P, Ma J, Wu T, Jones LL, Pei D, Cheng C, Geiger TL. Preferential Use of Public TCR during Autoimmune Encephalomyelitis. J Immunol. 2016; 196:4905–4914. [PubMed: 27183575]

Abbreviations

MOG	myelin oligodendrocyte glycoprotein
NFM	neurofilament medium protein

pMHC	peptide: MHC
2D	2-dimensional
CNS	central nervous system
EAE	experimental autoimmune encephalomyelitis
-/-	deficient synonymous with knockout
WT	wild type C56BL/6 mice

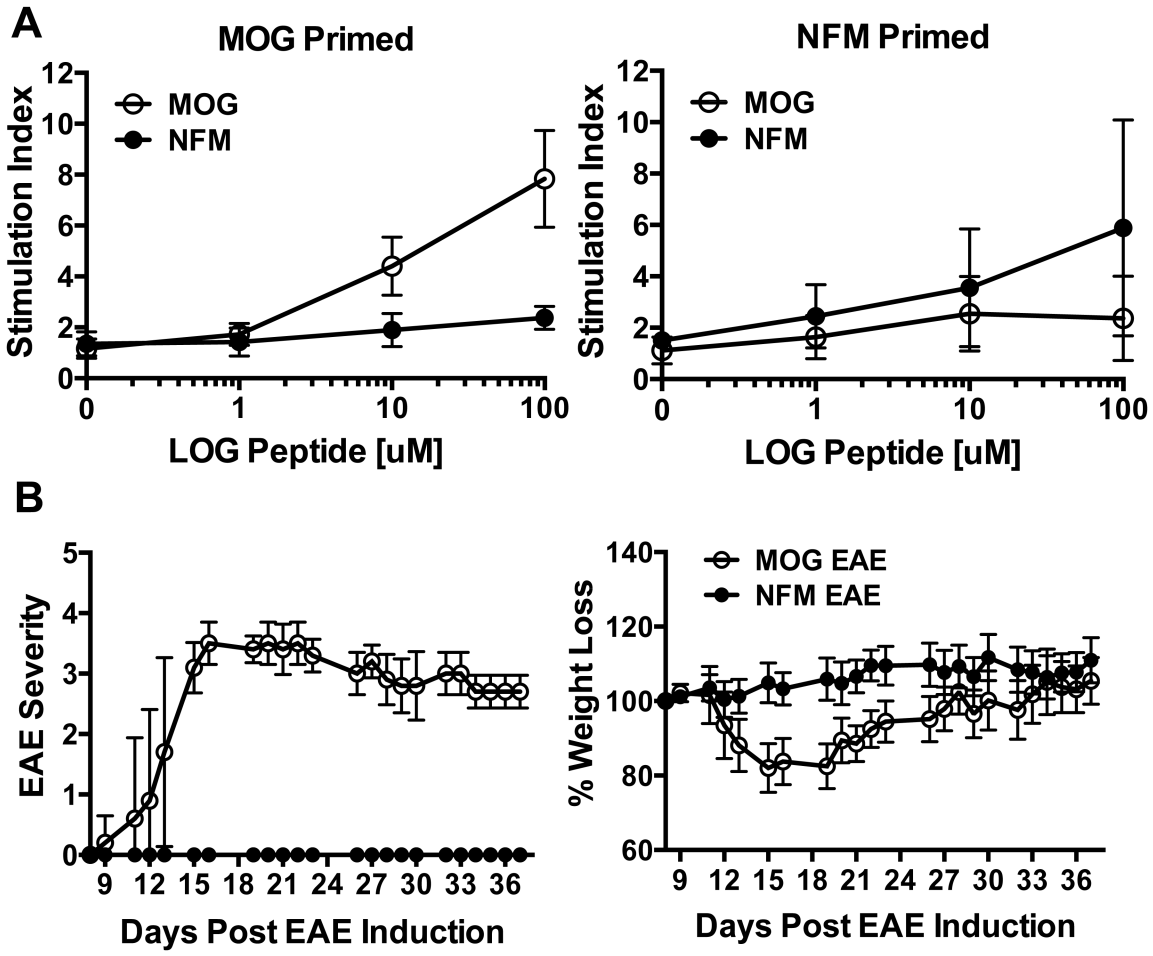

Figure 1. NFM is immunogenic but not encephalitogenic

A) Lymph nodes cells were harvested 12-14 days after priming C57BL/6 mice with MOG_{35-55} or NFM_{15-35} in CFA. Cells were directly assessed for antigen specific proliferation and ^{3}H-thymidine incorporation. Counts per minute were assessed and reported as stimulation index in order to average multiple experiments. Data is averaged from at least 3 experiments and 5 or more replicates per condition. B) EAE was induced in C57BL/6 mice using MOG_{35-55} (n=7) or NFM_{15-35} (n=15) with mice being monitored for paralytic severity and weight loss. Data is representative of 2 experiments.

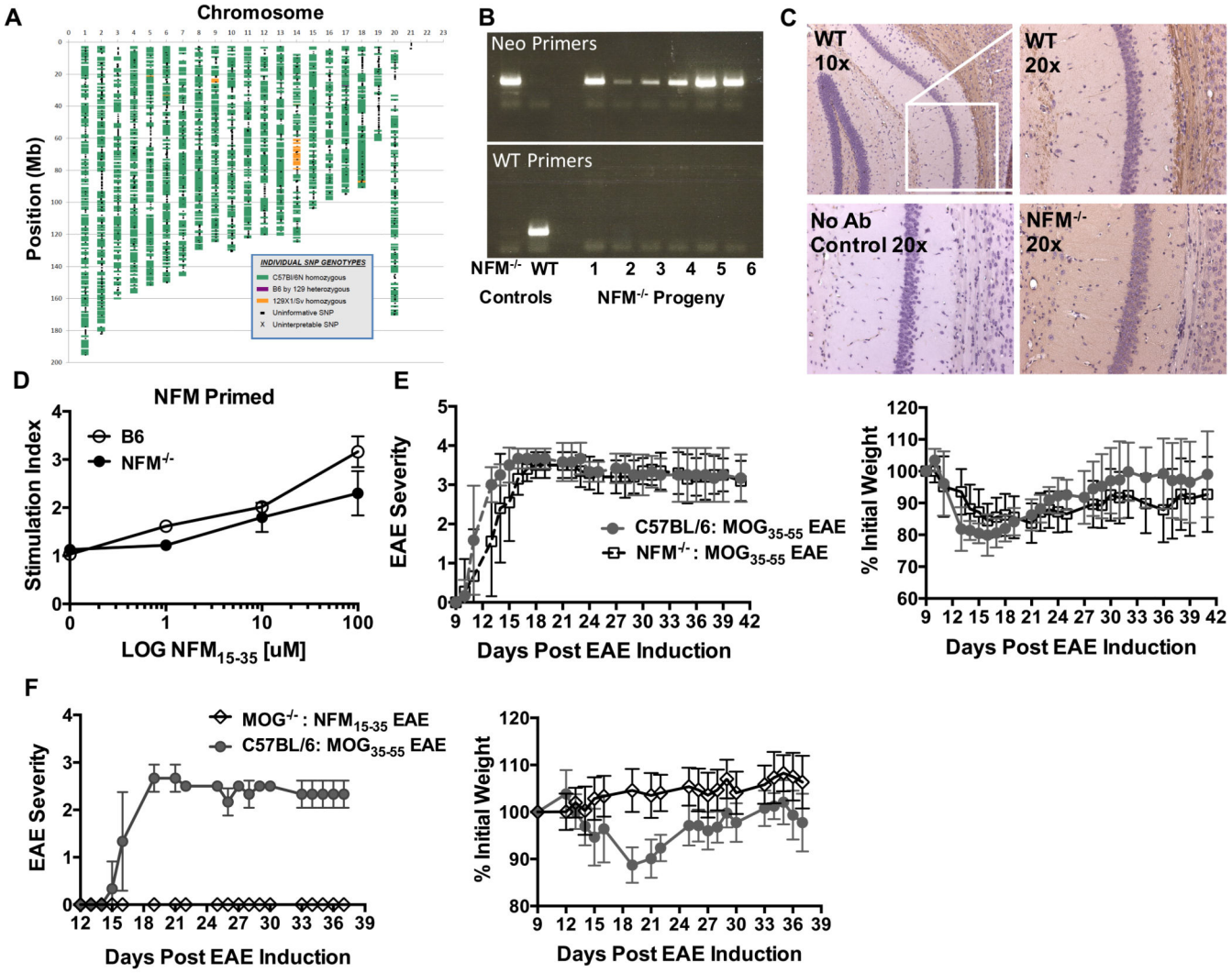

Figure 2. Characterization of NFM deficient mice suggests MOG is the critical autoantigen for induced EAE

A) Mice were backcrossed to C57BL/6 and confirmed by DartMouse to be 99% C57BL/6N (n=3) with analyses of 1 mouse shown. SNPs from C57BL/6N are shown in green and variances are highlighted in yellow (129X 1/Sv) or pink (heterozygous for C57BL/6N and 129). B) WT control mice or progeny of the $NFM^{-/-}$ backcross to C57BL/6 were individually PCR tested for the presence (Neo Primers) or absence (WT Primers) of the neomycin cassette disrupting exon 1 of *Nefm*, shown are 2 representative gels. C) Representative light microscopy images (10× or 20× magnification) of the pyramidal cell layer in the hippocampus of WT C57BL/6 mice versus $NFM^{-/-}$ mice. NFM expression was evaluated by immunostaining with NFM specific antibody NN18 (Millipore MAB5254) and compared to control slides where the primary antibody was withheld. NFM (dark brown) was visualized in cell bodies and fiber tracts of WT mice (n=1) but not $NFM^{-/-}$ mice (n=2). Sections were counterstained with hematoxylin (blue/purple) to highlight nuclei. D) Lymph nodes cells were harvested 12-14 days post NFM_{15-35} / CFA priming of C57BL/6 or $NFM^{-/-}$ mice. Counts per minute were assessed 24 hours after the addition of ^{3}H-thymidine. Data is the

average of 2 replicates per condition. E) MOG_{35-55} EAE was induced in WT and $NFM^{-/-}$ mice with disease course and weight loss were subsequently monitored. The data here represents 1 of 3 experiments with a total of n=10 WT mice and n=28 $NFM^{-/-}$ mice. There was no significant difference in day of symptom onset p=0.093 using an unpaired, nonparametric T test with Mann-Whitney post hoc test. F) $MOG^{-/-}$ mice were challenged with a NFM_{15-35} EAE induction in order to assess ability of T cells to recognize NFM alone and cause EAE, n=19. WT mice were challenged with MOG_{35-55} as a positive control n=5. Data shown is representative of 2 experiments.

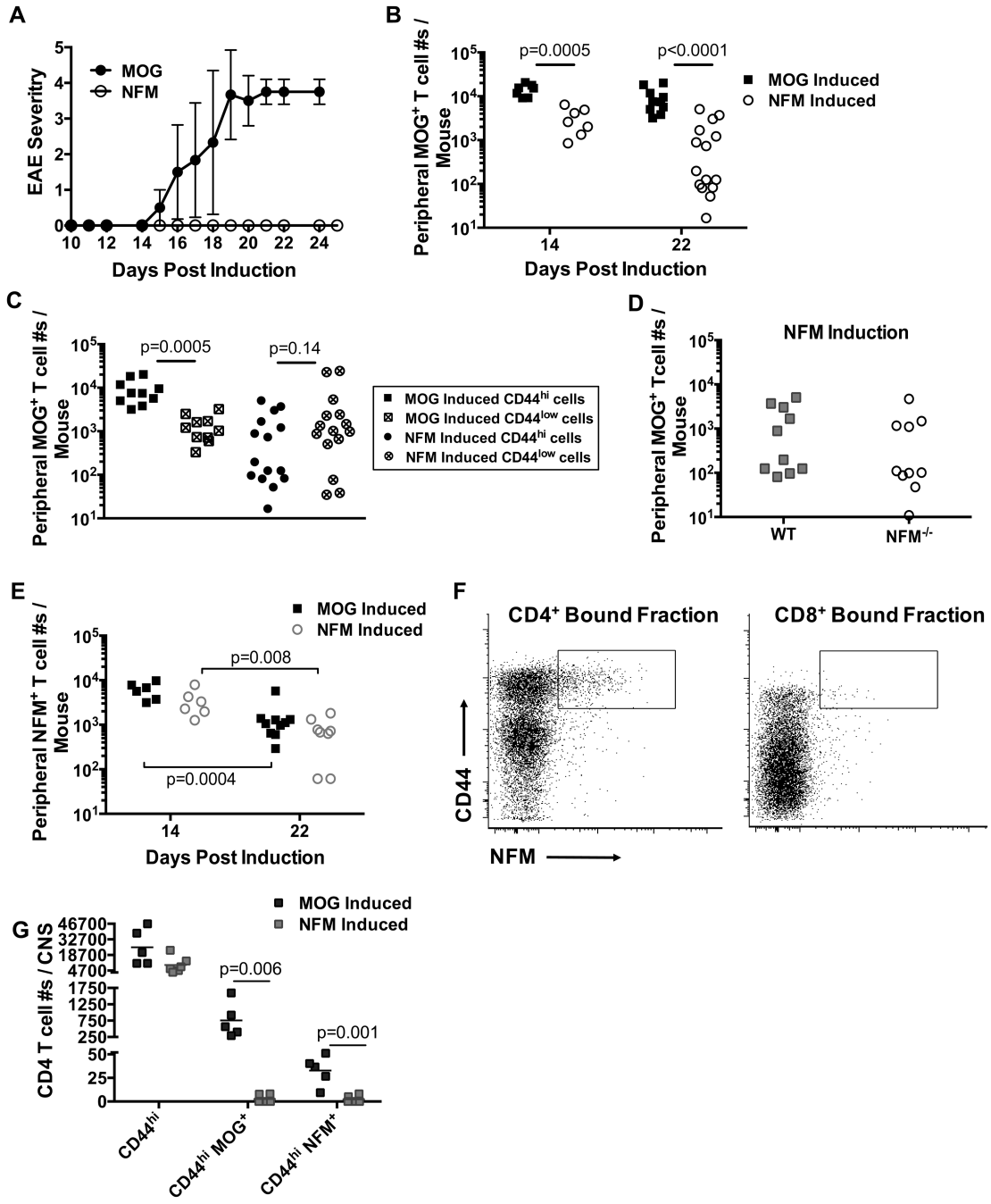

Figure 3. MOG specific T cell expansion is poor after NFM challenge

A) EAE was induced in IFNγ receptor knockout mice after MOG_{35-55} (n=6) or NFM_{15-35} (n=14) challenge. Disease course is representative of 2 experiments. B) WT mice were induced with an EAE challenge of MOG_{35-55} or NFM_{15-35} in CFA plus pertussis toxin. MOG_{38-49} or NFM_{18-30} tetramer pulldowns were performed on days 14 (n=6-7 mice / group) or 22 (n=8-15 mice / group) post challenge. MOG_{38-49} detection of $CD4^+$ $CD44^{hi}$ T cells differed significantly between MOG_{35-55} and NFM_{15-35} induction 14 or 22 days post injection. $CD4^+$ T cells were identified with an initial lymphocyte gate (FSC-A / SSC-A)

followed by a singlet gate (SSC-W / SSC-H), $CD3^+$ $CD11b^-$ $CD11c^-$ $CD19^-$ gate and $CD4^+$ versus $CD8^+$ gate. C) Day 22 T cell activation status was evaluated by observing the number of activated $CD44^{hi}$ versus unactivated $CD44^{low}$ MOG specific T cell numbers. NFM_{15-35} induction did not significantly induce the numbers of $CD44^{hi}$ MOG specific T cells ($p<0.0001$) expanded by MOG_{35-55} induction. D) WT or $NFM^{-/-}$ mice were challenged with NFM_{15-35} in CFA, as in (A). 22 days later, no significant differences were found in expansion of MOG_{38-49} T cells between WT and deficient mice (n=10 / strain, p=0.41). E) No significant differences in NFM_{18-30} detection were seen between MOG_{35-55} versus NFM_{15-35} induction groups at d14 (p=0.09) or d22 (p=0.25). Representative flow plots from the bound fraction of the tetramer enrichment at d14 post challenge are shown (F). G) MOG_{38-49} tetramer was used to identify antigen specific T cells in the CNS of 5-6 mice / group d22 after induction. There was no significant difference seen in the $CD3^+$ $CD4^+$ $CD44^+$ population p=0.06 despite significant differences in enumerating MOG and NFM tetramer positive cells. All statistics were done using 2-tailed unpaired, parametric t tests assuming both populations had equal standard deviations.

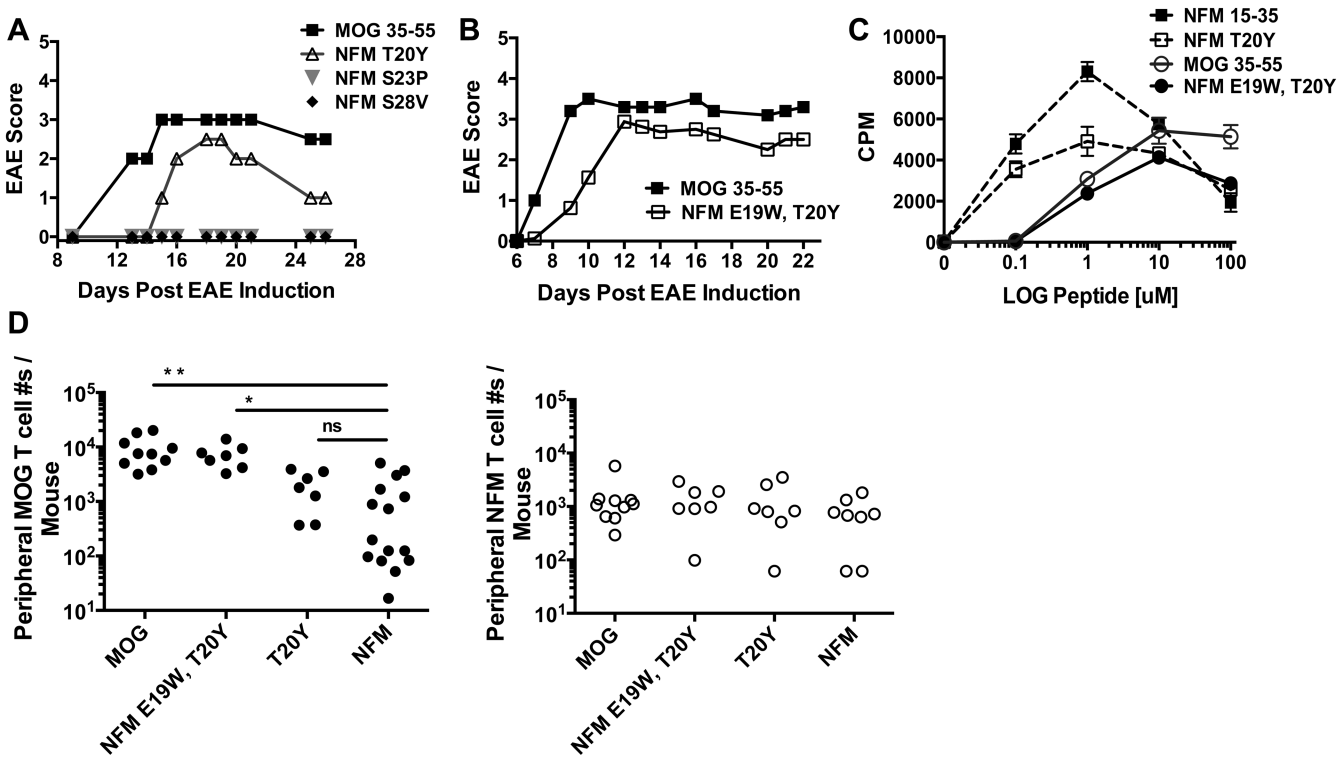

Figure 4. NFM variants at amino residues P1 and P-1 restored MOG_{38-40} tetramer detection and encephalitogenic incidence to 100%

A) Synthesized variant peptides of NFM_{15-35} were used to induce EAE in C57BL/6 mice and disease course was monitored (panels A-B and Table II). Panel A is the graphical version of Exp. 1 and panel B is the graphical version of Exp. 5 detailed in Table II. The experiments represented in A-B were performed 2 times. C) 2D2 T cell dose response curves for NFM_{15-35}, MOG_{35-55} and NFM variants. This experiment was performed 1 time in duplicate. D) MOG specific T cell numbers from the periphery at d22 post challenge were enumerated with MOG_{38-49} and NFM_{18-30} tetramers. Statistics between indicated peptide challenges were performed with 2-tailed unpaired, parametric t tests with the following designations ** $p<0.0001$ with F test variance $p<0.0001$, * $p<0.0001$ with F test variance of $p=0.01$ and T20Y versus NFM_{15-35} was not significant with $p=0.245$ and F test variance $p=0.857$. MOG_{35-55} versus 'NFM E19W, T20Y' has $p=0.455$ and exhibited no significant differences in means or F test variances. Expansion of NFM specific T cell numbers in the periphery were also assessed and no overall differences were seen by ordinary one-way ANOVA $p=0.63$.

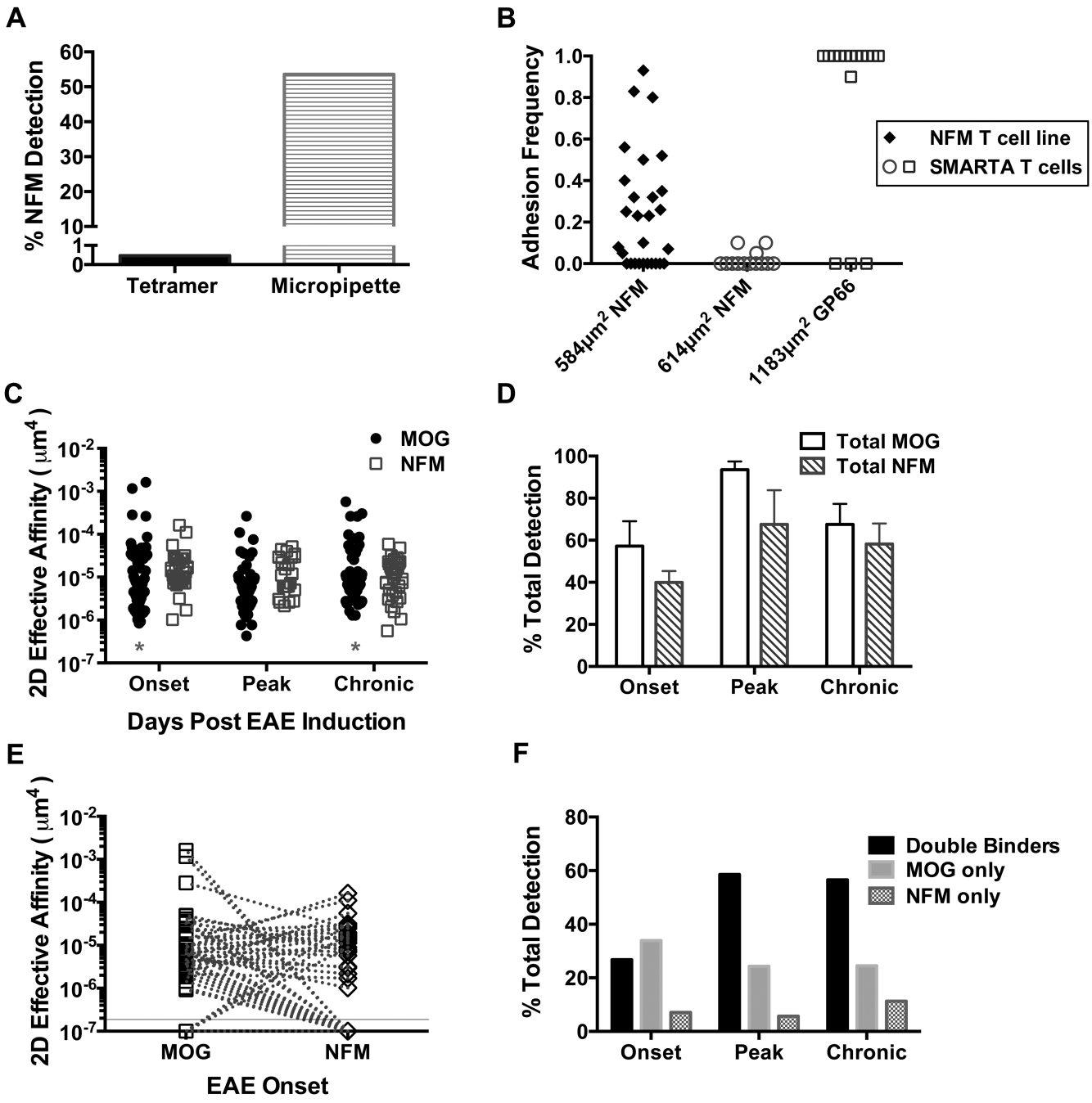

Figure 5. CNS T cell infiltrates that recognize NFM_{18-30} are largely specific for MOG_{38-49}

A) Splenocytes from a mouse primed with NFM_{15-35} were cultured for 1 week and tested for NFM_{18-30} specificity by tetramer (A) or the 2D micropipette adhesion frequency assay with n=28 cells. B) NFM specificity of the 2D micropipette adhesion frequency assay was shown via comparison to LCMV specific SMARTA T cells cultured on GP_{66-80} (n=16 cells). Densities of the NFM_{18-30} or GP_{66-77} I-A^b monomers coated on the RBC sensor are reported on the x-axis and each symbol represents one T cell. C) EAE was induced with MOG_{35-55} and $CD4^+$ T cells were isolated from the CNS at indicated time points where

'onset' designates days 12-16 (n=56 cells), 'peak' days 20-23 (n=70 cells), and 'chronic' days 28-32 (n=53 cells) post induction. Each dot represents one T cell. Log transformed affinities were analyzed by two-tailed, unpaired parametric t-tests with assumption of equal standard deviations were used to compare MOG_{38-49} versus NFM_{18-30} specific T cells at each time point; onset (p=0.51), peak (p=0.058) and chronic (p=0.55). Asterisks mark significant differences in population breadth between MOG_{38-49} and NFM_{18-30} specific T cells at onset (p=0.004) and chronic (p=0.029) disease using unpaired, parametric t tests with F tests to compare variances. D-F) Breakdown of the data collected in (C). D) Bar graphs indicate the average percent of detection among the individual T cells analyzed per 2D micropipette experiment; average experiments include 7 for onset, 4 for peak and 5 for chronic time points. No significant difference was seen between MOG and NFM specific detection using a two-tailed paired t tests $p>0.1864$. E) Each dotted line links one individual T cell between its affinities for MOG_{38-49} versus NFM_{18-30}. Zero binding of a T cell to a given antigen could not be graphed on a log-scale and were given an arbitrary value of 1×10^{-7} and are graphically visualized below the solid y-intercept line. F) Breakdown of individual T cell specificity for one or both antigens using the data in panel D. Double binders is a category of cells that recognize both MOG_{38-49} and NFM_{18-30}.

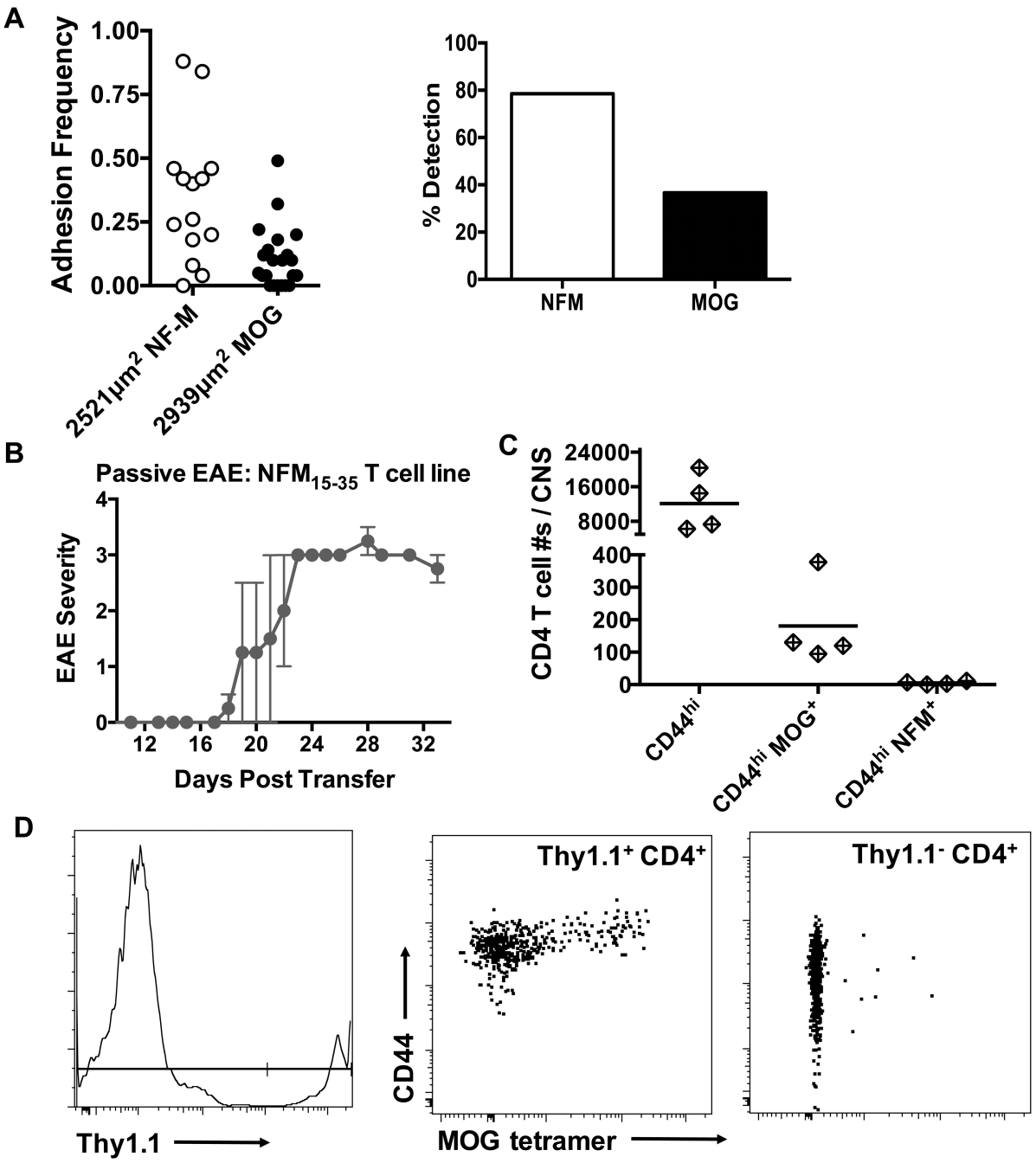

Figure 6. Encephalitogenicity of a NFM T cell line is concomitant with infiltration of tetramer positive MOG specific T cell in the CNS

A) Lymph nodes from NFM_{15-35} primed C57BL/6 wild type mice were harvested and cultured for 1 week on NFM_{15-35}. 2D micropipette adhesion frequency assay was used to assess MOG versus NFM specificity. This figure represents one of 2 experiments, displaying data from 36 cells. B) Irradiated (400 rads) C57BL/6 mice received 10×10^6 cells from a NFM T cell line (i.p.). 25 days post transfer, the CNS of mice with scores from 1.0 to 3.5 were harvested and antigen specificity was quantitated with MOG_{38-49} or NFM_{18-30} tetramer (C). D) Representative flow plots from adoptive transfer of a $Thy1.1^+$ NFM T cell

line in to a Thy1.2 recipient. C & D are data representative from 1 of 2 experiments. All statistics were done using 2-tailed unpaired, parametric t tests assuming both populations had equal standard deviations.

Table I

Amino acid sequences of MOG_{35-55}, NFM_{15-35} and NFM_{15-35} variant peptides. The nine core amino acids (P1-P9) are denoted along with P-1. Substitutions in NFM_{15-35} were made at P-1, P1, P4, and P9

	-1	1	2	3	4	5	6	7	8	9								
NFM 15-35	R	R	V	T	E	T	R	S	S	F	S	R	V	S	G	S	P	S	S	G	F
MOG 35-55	***M***	***E***	***V***	***G***	***W***	***Y***	***R***	***S***	***P***	***F***	***S***	***R***	***V***	***V***	***H***	***L***	***Y***	***R***	***N***	***G***	***K***
NFM T20Y	R	R	V	T	E	***Y***	R	S	S	F	S	R	V	S	G	S	P	S	S	G	F
NFM E19W, T20Y	R	R	V	T	***W***	***Y***	R	S	S	F	S	R	V	S	G	S	P	S	S	G	F
NFM S23P	R	R	V	T	E	T	R	S	***P***	F	S	R	V	S	G	S	P	S	S	G	F
NFM S28V	R	R	V	T	E	T	R	S	S	F	S	R	V	***V***	G	S	P	S	S	G	F

J Immunol. Author manuscript; available in PMC 2018 October 15.

Table II

Summary table of EAE experiments with NFM variant peptides compared to MOG_{35-55}

Synthesized variant peptides of NFM_{15-35} were used to induce EAE in C57BL/6 mice. Disease was monitored in experimental mice (N) and percent incidence of disease along with average day of symptom onset and maximal disease score +/- standard deviations are reported. Disease incidences after challenge with MOG_{35-55} versus T20Y were summarized in the combined (Exp. 1 & 2) section.

Exp. #	Peptide	N	% Incidence	Avg. Day Onset	Avg. Max Score
1	**MOG 35-55**	**2**	**50**	**13**	**3**
	NFM T20Y	**2**	**50**	**15**	**2.5**
	NFM S23P	**2**	**0**	**-**	**-**
	NFM S28V	**2**	**0**	**-**	**-**
2	**MOG 35-55**	**2**	**100**	**14.5 +/- 0.7**	**3 +/- 0.7**
	NFM T20Y	**4**	**25**	**32**	**2.5**
	NFM S23P	**2**	**0**	**-**	**-**
	NFM S28V	**2**	**0**	**-**	**-**
Combined Exp. 1 & 2	*MOG 35-55*	*4*	*75*		
	NFM T20Y	*6*	*33.3*		
3	**MOG 35-55**	**3**	**100**	**10 +/- 3.5**	**3.7 +/- 0.29**
	NFM E19W, T20Y	**5**	**100**	**10.6 +/- 1.5**	**2.5 +/- 1.2**
4	**MOG 35-55**	**5**	**100**	**8.2 +/- 1.1**	**3.9 +/- 0.22**
	NFM E19W, T20Y	**8**	**100**	**10.3 +/- 2.0**	**3.3 +/- 0.46**